PARAMETRIC ANALYSIS OF ADJACENT PRESTRESSED CONCRETE BOX-BEAMS WITH UHPC-DOWEL SHEAR KEYS

Eric Steinberg, PhD, PE, Professor, Civil Engineering, Ohio University, Athens, OH
John Ubbing, Grad. Research Asst., Civil Engineering, Ohio University
Oliver Giraldo-Londoño, Grad. Research Asst., Civil Engineering, Ohio University
Ali Semendary, Grad. Research Asst., Civil Engineering, Ohio University

ABSTRACT

A parametric study on the behavior of a pair of adjacent box-beams coupled together with an ultra-high performance concrete (UHPC) shear key, and transverse dowel bars equally spaced along the shear key length was conducted using ABAQUS. Two shear key configurations different than the standard shear key were investigated: 1) a partial-depth UHPC shear key; and 2) a full depth UHPC shear key. For both cases, the spacing of transverse dowel bars was varied, and temperature gradient through the beams' cross section was included. These models investigated the loading transfer between beams as well as the forces developed in both the shear key and transverse dowel bars. Results from this research helped to understand the performance of the longitudinal UHPC shear key and the capability of the dowel bars to transfer loads. The models with partial-depth shear key were compared to active testing at the Turner-Fairbank Highway Research Center (TFHRC) for verification. This was with the aim of exploring nominal dowel bar spacing and aid in the design of a short span bridge in Fayette County, Ohio that will utilize similar UHPC partial depth shear keys in its prestressed concrete box beam design.

Keywords: Adjacent Box-Beams, Dowel Bars, UHPC

INTRODUCTION

Adjacent box-beam bridges have been widely used in the United States for decades. This type of bridge has been used for the construction of short and medium span bridges, since it has shown to be economical and practical [1]. The superstructure is constructed by placing box-beams next to each other until the full width of the bridge is reached. Once this is completed, shear keys are cast between beams, and in some cases, when the shear keys are cast, transverse post-tensioning and/or a cast in place concrete deck are used to improve the load transfer between beams.

The shear keys are a fundamental part of the load transfer mechanism between adjacent beams. For this reason, it is essential to have a detailed understanding of their mechanical behavior. An extensive literature review has revealed that in current practice, this type of bridge has shown to be susceptible to longitudinal cracking along the shear keys. These cracks can propagate into the bridge's wearing surface due to loading and thermal cycles, allowing water and other chemicals to penetrate between the beams, causing corrosion of reinforcement, and concrete staining and spalling [1][2]. Based on the continued issues related to the shear keys, it is inferred that complete understanding of the mechanical behavior of the shear keys has not been currently achieved, and for this reason, more research needs to be conducted.

The use of Ultra-High Performance Concrete (UHPC) for the construction of more durable and resilient shear keys has been an approach recently implemented by the Federal Highway Administration (FHWA) and several Departments of Transportation (DOT). Several research projects have been conducted where UHPC was studied in multiple applications [3][4][5]. One of these research projects focused on studying the performance of field-cast UHPC shear key connections for applications in precast concrete bridge deck panels under static and cyclic loadings. In this project, different specimens were fabricated to study both longitudinal and transverse connections. As part of this study, different reinforcing details transversely crossing the shear keys (i.e., straight lapped bars, headed bars, and intersecting hoop bars) were implemented in the specimens. Results from this research revealed sufficient performance related to cracking under cyclic loading as well as exceptional bonding strength in the interface between the UHPC connection and the concrete deck panels [3].

A more recent study presented several recommendations for the design and construction of field-cast UHPC connections. Construction recommendations covered topics such as component preparations, formwork, mixing and placing, curing, surface profiling, and material testing [4]. Additional research by Steinberg et al.[5] discussed, among other aspects, the finite element modeling of both a pair of adjacent box-beams and a full adjacent box-beam bridge, using partial and full depth UHPC shear key connections with dowel bars embedded in box-beams that protruded into the shear key. Results from these models showed that transfer of loads between adjacent beams was satisfactory when using UHPC-dowel shear key connections.

Some of the research previously discussed considered steel bars transversely crossing the grouted joints [3][5]. The interaction between these steel bars and the cementitious material surrounding them (e.g., grout or UHPC) allows the development of a mechanism called dowel action. This mechanism has been extensively studied, and is known to be a factor contributing in

the shear force transfer in reinforced concrete structures [6][7]. This mechanism is the result of reaction forces between the dowel bars and the surrounding concrete. These reaction forces are obtained when there is lateral displacement of the dowels due to differential deflections between adjacent beams. However, there has not been a detailed analysis of the behavior of the dowels and their contribution in the mechanism of load transfer between adjacent box-beams.

Different researchers studied the mechanism of dowel action for different applications [6][7]. One of these studies focused on experimental and analytical investigations of the dowel action mechanism with emphasis in offshore structures [6]. All the formulations in this research work were based upon the concrete stress distribution under the dowel, as proposed by Ramussen [7]. In this research, the mechanism of dowel action was studied for concrete structures subject to both monotonically increasing loads and cyclic loads. Results showed that the number of cycles before failure in the dowels decreased exponentially as the applied shear stress-to-static shear strength ratio increased. Ultimate dowel capacity, on the other hand, was proven to increase as the diameter of the dowel, concrete compressive strength, and steel yielding stress increased. However, ultimate dowel capacity was shown to decrease when axial stresses in the dowel approached the steel yielding stress.

The purpose of this research was to perform a parametric study on the behavior of a pair of adjacent box-beams connected by an ultra-high performance concrete (UHPC) shear key and transverse dowel bars equally spaced along the shear key length using ABAQUS. Two shear key configurations different than the standard shear key were investigated: 1) a partial-depth UHPC shear key; and 2) a full depth UHPC shear key. For both cases, the spacing of transverse dowel bars was varied, and a temperature gradient through the beams' cross section was included. Results from this research helped to understand the performance of the longitudinal UHPC shear key and the capability of the dowel bars to transfer loads. The models with a partial-depth shear key were compared to active testing at the Turner-Fairbank Highway Research Center (TFHRC) for verification and calibration. This was done with the aims of exploring nominal dowel bar spacing and contributing to the design of a short span prestressed concrete box beam bridge in Fayette County, Ohio that will utilize similar UHPC partial depth shear keys.

MODEL CONSTRUCTION

Each finite element model was designed using Abaqus/CAE software and was analyzed as a linear three-dimensional model. The first set of models, involving a partial depth UHPC shear key connecting two adjacent box beams, were developed to compare their performance with experimental data collected from laboratory testing conducted at the TFHRC. These models also investigated how varying the spacing of the transverse dowel bars protruding through the UHPC shear keys as well as a positive temperature gradient affected the load transfer performance between beams. The second set of models was similar to the first, but incorporated full depth UHPC shear keys. These models were not compared to TFHRC testing due to a lack of experimental data, but they investigated the same parameters as the first set of models to compare performance differences between partial and full depth doweled UHPC shear keys.

GEOMETRY

The dimensions and specifications for the partial depth shear key models were provided by the TFHRC, as shown on the right side of Figure 1. The shear key for these models had the same dimensions as the shear key of the bridge to be built in Fayette County, Ohio as shown in Figure 1 (left). As shown in **Error! Reference source not found.**, the shear keys used in these models are wider and have unique dimensions that are different from standard shear key dimensions used in Ohio. In addition, the overall beam designs are similar despite the Fayette County beam's shallower height and larger width. Due to these similarities, results gathered from the finite element models discussed in this section aided in determining the performance expectations of the UHPC shear key to be used in Fayette County.
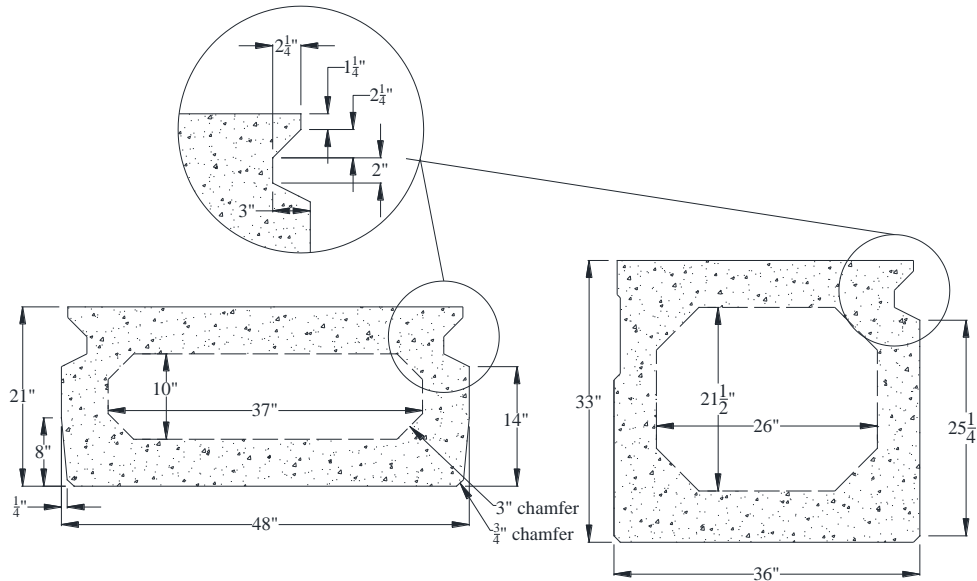
Fig. 1 Preliminary dimensions of a Fayette County box beam (left); and the TFHRC testing subject's actual dimensions (right)

The second set of models were constructed using two adjacent box beams connected by a full depth UHPC shear key as shown in Figure 2. The dimensions of each beam and the shear key used in these models were also provided by the TFHRC.
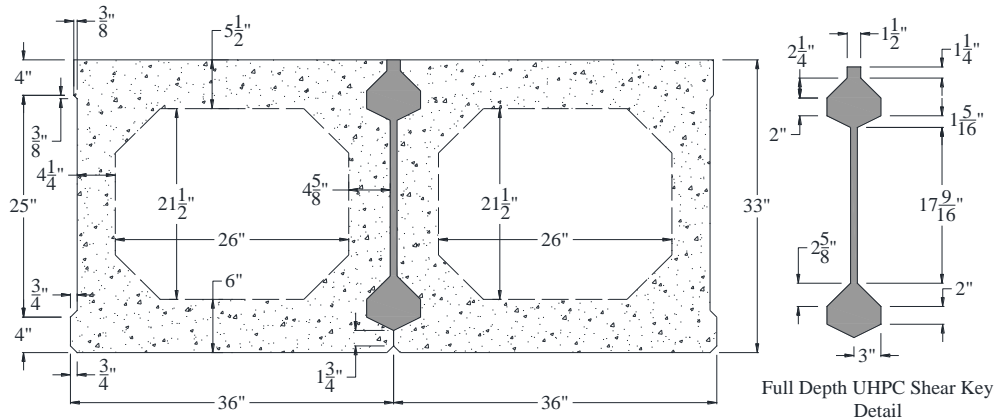
Fig. 2 Beams' cross sections and shear key detail for models with full depth UHPC shear key

All models incorporated transverse dowel bars that protruded 5.5 in. into the shear key. For the partial depth shear key models, the dowels were placed 4 in. below the top surface of the beams. The full depth shear key models utilized dowel bars in the top and bottom portions of the shear key. The top dowel bars were located 4" below the top surface, and the bottom dowels located 5 in. above the bottom surface. For all models, the dowel bars were spaced at staggered intervals equal to the TFHRC testing (i.e., spacing of 4 in.), then 6 in. and 12 in. apart as shown in Figure 3.
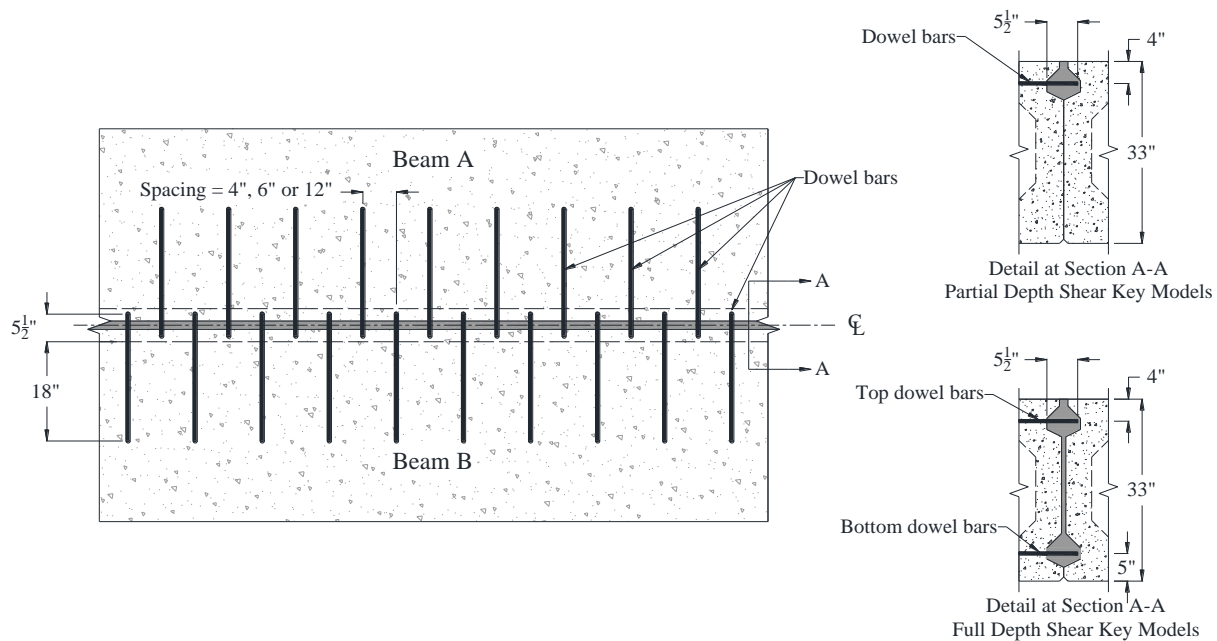
Fig. 3 Transverse dowel bars spacing (plan view)

Both of the box beams in each set of models consisted of a 50 ft. span with diaphragms at each end and at third points along the beams' span, longitudinal reinforcement, a shear key made of UHPC, transverse dowel bars, loading plates, and several bearing plates, as shown in Figure 4. All the parts were modeled as solid, deformable, three dimensional parts with linear elastic properties according to material testing at the TFHRC.
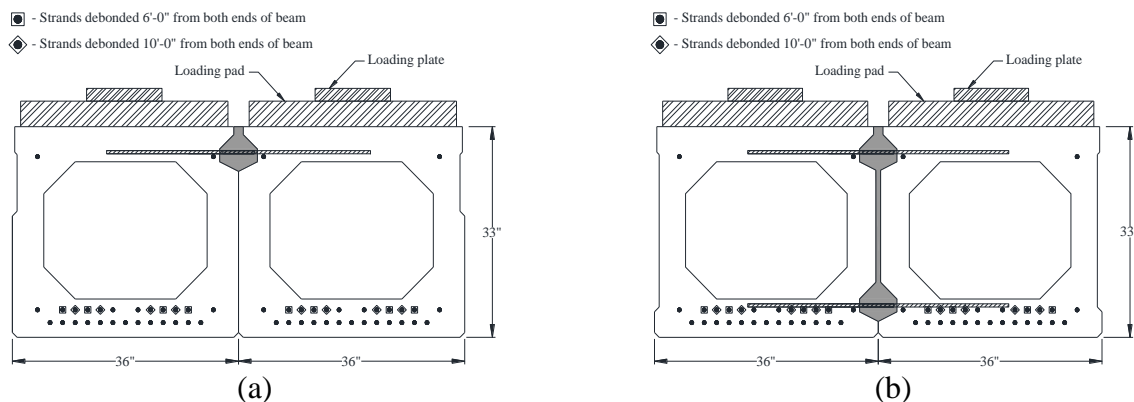
Fig. 4 Cross section view of models: (a) partial depth UHPC shear key models; and (b) full depth UHPC shear key models

PRESTRESSING FORCE AND SELF-WEIGHT

In each finite element model, the longitudinal reinforcement was embedded into each concrete beam and the effects of debonding and prestressing were included. According to the TFHRC, eight strands were debonded (four strands with a debonding length of 6 ft. and four strands with a debonding length of 10 ft.), as shown in Figure 4. This debonding was simulated by cutting each of these strands to its respective debonding length (6 ft. or 10 ft.) since stresses would not be transferred from the strands to the box beams in the these zones. Prestressing forces were created by applying a negative temperature to the prestressing strands through a predefined temperature field. Next, a body force was applied by selecting the entire model (i.e., beams, diaphragms, reinforcement, shear key), and then applying a "Body Force" in the negative y-direction. This "Body Force" value was found using a unit weight of reinforced concrete equal to 150 pcf.

Each model's prestressing was then verified by investigating the average maximum principle stresses and the stresses in the strand's parallel direction after the model had been analyzed with only the body and predefined temperature change applied. Once the verification was completed, the average maximum principal stresses and stresses in the strand's parallel direction that were approximately 155 ksi.

MATERIALS AND MESHING

Since every part was modeled as linear elastic, the material properties required for the model were Young's modulus, Poisson's ratio, and thermal expansion coefficient. A summary of these properties that were applied to each finite element model's parts are shown in Table 1. Values for Young's modulus and Poisson's ratio were collected from experimental testing conducted at the TFHRC. The thermal expansion coefficients for concrete and steel were obtained from PCI [9] and these values for UHPC were retrieved from a recent UHPC report [10].

Table 1: FEM material properties

Part	Young's Modulus (ksi)	Poisson's Ratio	Thermal Expansion Coefficient, α ($\times 10^{-6}$ in/in/°F)
Beams	5,650	0.20	6.0
UHPC Shear Key	7,590	0.18	8.5
Steel Components	29,000	0.30	6.0

Once material properties were applied to each part, they were assigned a mesh. Every part used in the models was created using C3D8R elements, which are considered by Abaqus as being eight node linear brick reduced integration hourglass control elements. There were a variety of seed numbers along each of the model's axis' due to varying partitions and the limitations of the Abaqus student license used for this research, which only allowed 100,000 nodes.

BOUNDARY CONDITIONS & INTERACTIONS

Each model included several boundary conditions that matched the conditions that were applied to the TFHRC's experimental testing of these box beams. The bottom portion of each beam's ends were attached to a large steel plate, which was attached to a smaller steel plate, as shown in Figure 5 (a-b). A line of nodes in along the x-axis in the center of each bottom bearing plate were restrained in either a pinned or roller condition and the remaining nodes were connected to the "ground" through a series of springs as shown in Figure 5 (a-b).

These springs partially restricted the node's fixed end rotation and were selected to "connect points to ground". Each spring was assigned a stiffness constant of 0.05, which was based of model calibration involving the agreement of experimental and analytical midspan deflections. The four thinner plates at the top of each of the beam's ends applied a downward pressure that reflected the experimental beam's clamped ends, which restricted their rotation while being loaded. This was implemented by the TFHRC to create stiffer end conditions, in order to induce higher stresses in the shear key, because previous experimental testing showed absence of shear key cracking.

(a)   (b)
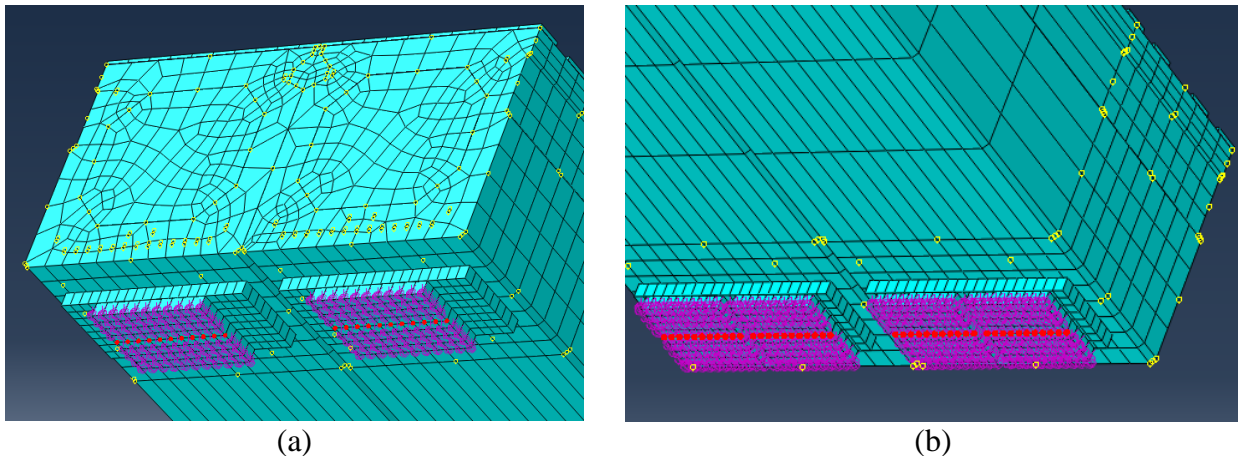
Fig. 5 Bearing steel plates used to apply boundary conditions: (a) left end's bearing plates; and (b) right end's bearing plates (pinned-fixed nodes are shown in red and springs are purple)

LOADING

The loading arrangement for the models was based on the TFHRC experimental testing. In this testing the loads were applied through four separate 12" by 12" steel plates located on top of the beams and at the beam's midspan as shown in Figure 4 (a-b). These four plates were placed on top of another set of larger and thicker plates in order to distribute the load uniformly, thus preventing any crushing of the box beam's top flanges.

According to the TFHRC experimental testing, the beams were loaded with a cyclic load that followed the pattern shown in Figure 6. During this procedure, one beam would begin at the lowest load, then receive gradually increasing load, while the opposite beam would begin at the largest load and continue to be unloaded. All the models were loaded using this same loading pattern. However, only one loading cycle was implemented in the models.
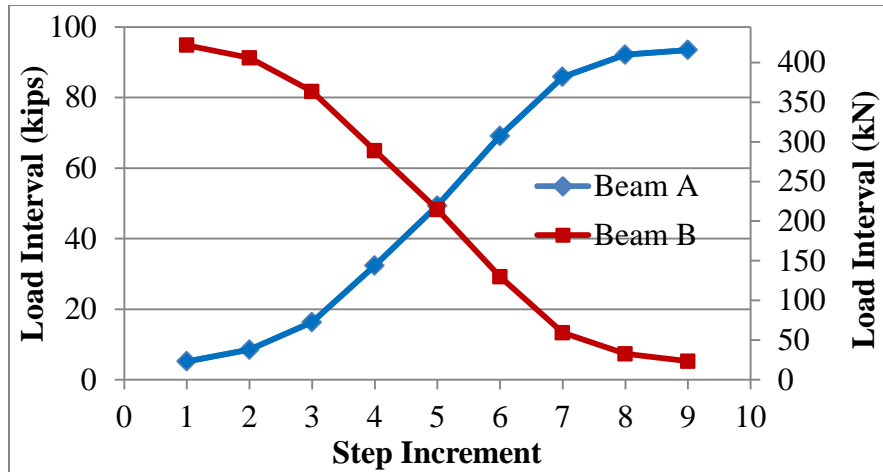
Fig. 6 Partial depth UHPC shear key cyclic loading procedure followed in experimental and analytical testing

APPLICATION OF TEMPERATURE GRADIENT

A positive temperature gradient according to AASHTO 2010 was applied in all the models. This gradient considered temperatures varying linearly from T_1 to T_2 in the first 4". of beam's depth measured from the top surface, and from T_2 to zero in the next 12", as shown in Figure 7. The values for $T_1 = 41$ °F and $T_2 = 11$ °F were selected according to the map of solar radiation zones for the United States (i.e., Figure 3.12.3-1; AASHTO, 2010) [8]. This temperature gradient was implemented in Abaqus through a predefined temperature field. The distribution pattern for the temperature gradient was obtained using a mapped analytical field.
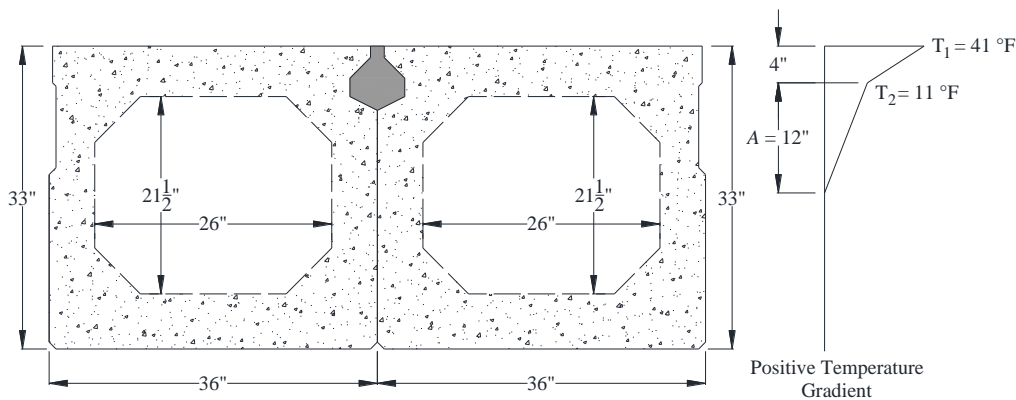
Fig. 7 Positive temperature gradient according to AASHTO 2010

RESULTS

MIDSPAN DEFLECTIONS

The first results studied were the midspan deflections. These deflections were used to validate all the finite element models. This validation was done by computing the percentage difference between the deflections obtained from the TFHRC and the deflections obtained from

the Finite Element (FE) models. According to the experimental setup by TFHRC, four nodes were selected to measure the vertical deflections at the beams' midspan. These nodes were located at each bottom corner of the beams cross section, and labeled Nodes 1, 2, 3, and 4, as shown in Figure 8. These nodes corresponded to the location of the LVDTs used by TFHRC to measure the midspan deflections.
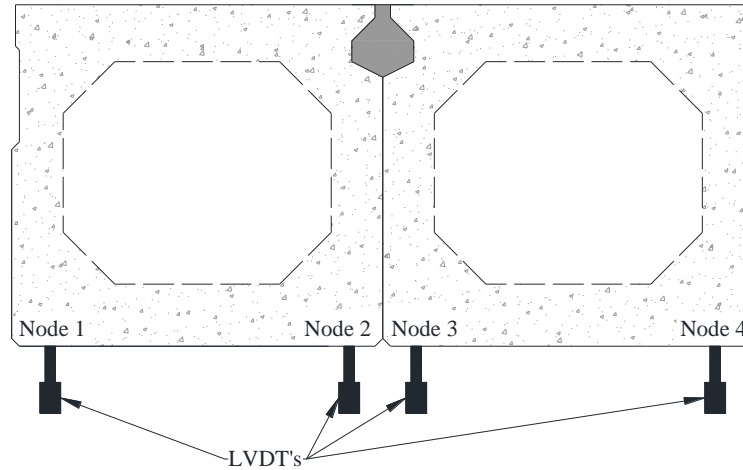
Fig. 8 Nodes used to measure the deflections at beams' midspan location

The results from the THFC as well as the deflections obtained from the FE models are shown in Table 2. As shown in Table 2, all percentage differences in the deflections at nodes 1, 2, 3, and 4 were between 0.1% and 3.6%, which indicates that all the input data (e.g., material properties, meshing, boundary conditions, and interactions) used to create the models accurately represents experimental results.

Table 2: FEM vs. TFCH experimental midspan deflections

Loading Beam A (kips)	Loading Beam B (kips)	THFC Experimental Deflections (in)				FE Models Deflections (in)				Percentage difference = [(Exp. - FEM)/Exp.]×100 (%)			
		Node 1	Node 2	Node 3	Node 4	Node 1	Node 2	Node 3	Node 4	Node 1	Node 2	Node 3	Node 4
5.2	94.8	0.362	0.372	0.378	0.396	0.355	0.365	0.382	0.398	2.2	2.1	1.1	0.5
8.5	91.2	0.360	0.369	0.374	0.391	0.355	0.364	0.380	0.396	1.3	1.2	1.7	1.2
16.3	81.7	0.362	0.367	0.372	0.386	0.353	0.360	0.372	0.385	2.4	2.1	0.1	0.2
32.4	64.9	0.367	0.367	0.371	0.378	0.358	0.360	0.366	0.375	2.5	1.8	1.1	1.0
49.3	48.2	0.375	0.368	0.371	0.372	0.368	0.364	0.364	0.367	1.9	0.9	1.7	1.2
69.1	29.2	0.385	0.370	0.371	0.365	0.380	0.371	0.363	0.361	1.2	0.3	2.2	1.3
85.9	13.3	0.393	0.372	0.372	0.361	0.391	0.377	0.363	0.356	0.5	1.4	2.5	1.3
92.2	7.3	0.396	0.373	0.373	0.358	0.395	0.379	0.363	0.354	0.2	1.7	2.6	1.2
93.5	5.2	0.397	0.373	0.373	0.358	0.393	0.377	0.360	0.350	1.0	0.9	3.6	2.2

Once these models were validated, the same material properties, meshing, boundary conditions, and interactions were used to generate multiple finite element models. These additional models included changes in the dowel bar spacing and shear key configuration. After

all these models were generated, differential deflections between the two adjacent beams were studied for every load increment. The differential deflections were calculated by taking the absolute value of the difference between the midspan deflection at the inside edges of the pair of beams. The differential deflections were studied for different transverse dowel bar spacing and for models with a partial depth UHPC shear key and a full depth UHPC shear key. Figure 9 (a) displays the results obtained when no temperature gradient was applied to the models, and Figure 9 (b) shows the results obtained when a positive temperature gradient was applied to the models.

From Figure 9 (a-b), it was observed that the differential deflections between adjacent beams increased approximately linearly as the magnitude of the differential load (|Load A – Load B|) became larger. The results also show that as the dowel bar spacing increased, the differential deflections between adjacent beams became larger, for both the partial and full depth shear keys. In addition, results showed that differential deflections for models with full depth shear key were overall between 40% - 60% of the differential deflections obtained for models with partial depth shear key. However, for both the partial and full depth shear key models, the maximum differential deflection is within 0.02 in. [7] for the loading applied. Finally, the temperature gradient caused a slight reduction in the differential deflections.

(a)   (b)
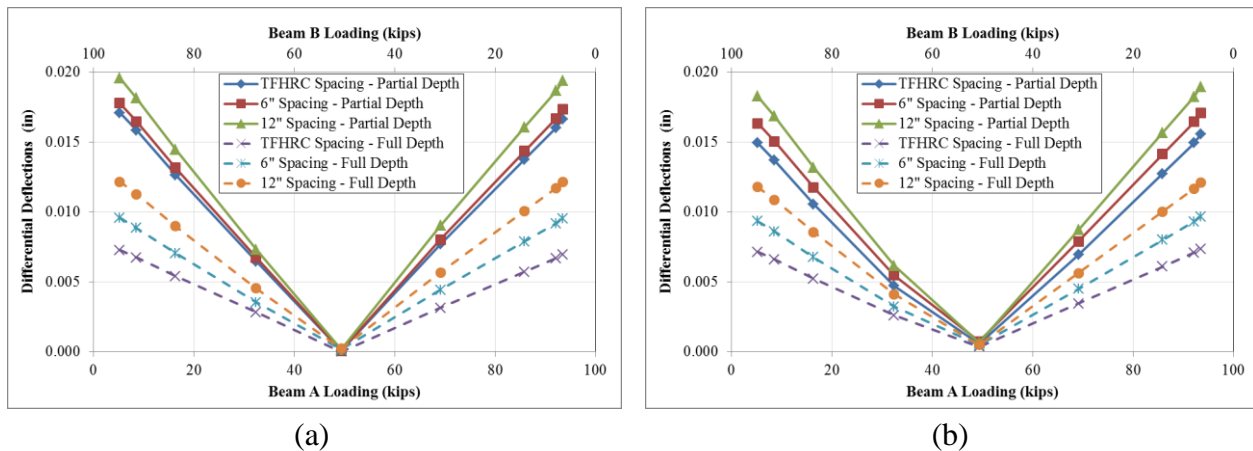
Fig. 9 Differential deflections between beams at midspan: (a) temperature gradient not applied; (b) temperature gradient applied

PRINCIPAL TENSILE STRESS IN SHEAR KEY

The maximum principle tensile stresses being produced in each shear key were explored next for the partial and full depth UHPC shear key models with and without the application of a temperature gradient. The comparisons of these stresses between the varying transverse dowel bar spacing and lengths are shown in Figure 10. As shown in Figure 10(a), the principal tensile stresses induced in the shear keys increased as the dowel bar spacing increased in the respective shear keys. When the temperature gradient was applied [Figure 10(b)], a similar relationship was produced, but on a smaller scale due to a reduction in the amount of maximum principle tensile stresses being produced in each shear key.

Overall, the finite element models incorporating full depth shear keys resulted in higher tensile stresses than the partial depth shear keys. The models with transverse dowel bars spaced at 12 in. within a full depth shear key also produced the highest amount of maximum principle

tensile stresses during each loading step regardless of whether or not the temperature gradient was applied. These stresses did not approach the UHPC's tensile strength shown in Eq. 1 when the temperature gradient was applied [10]. However, when there was no temperature gradient, the full depth shear key with dowel bars spaced at 12 in. exceeded this limit.

$$\text{Tensile Strength} = 6.7\sqrt{f'_c} = 1.04 \text{ ksi} \tag{Eq. 1}$$

where: f'_c = UHPC Compressive Strength = 24 ksi

Obtaining maximum principal tensile stresses exceeding the tensile strength of UHPC implied the need for nonlinear analysis if behavior beyond cracking was of interest. However, this was not the focus of the study as first crack formation was of greater concern. Therefore, 12 in. dowel spacing may result in issues with cracking while the other spacing and configurations should perform well. It should also be noted the UHPC to precast concrete interface may debond prior to UHPC tensile failure. The interfacial behavior is highly dependent on the surface preparation. Exposing aggregate by the use of a retarder on the precast section greatly enhances the bond performance as was done in the TFHRC testing.

(a)   (b)
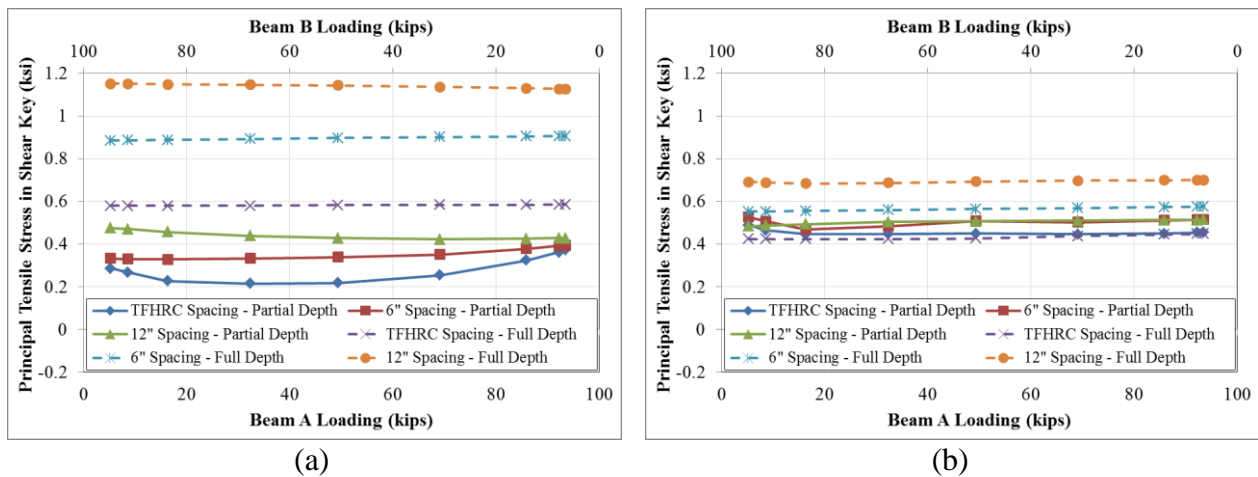
Fig. 10 Maximum principle tensile stress comparisons amongst the partial and full depth shear key's varying transverse dowel bar spacing: (a) temperature gradient not applied; (b) temperature gradient applied

PRINCIPAL TENSILE STRESS IN DOWEL BARS

The maximum principle tensile stress in the dowel bars was analyzed next. This data is displayed in Figure 11, which shows that as the dowel bar's spacing increased in each shear key regardless of a temperature gradient, the maximum principle stresses occurring in each set of bars also increased. In each dowel bar spacing case, the full depth shear key displayed higher stresses being produced in the dowel bars.

The full depth shear key finite element model with bars spaced at 12" exhibited the highest amount of maximum principle tensile stresses with or without a temperature gradient applied. However, the highest amount of maximum principle tensile stresses shown in Figure

11(a) or Figure 11(b) did not approach the yield strength of the Grade 60, #4 rebar transverse dowel bars.

(a)   (b)
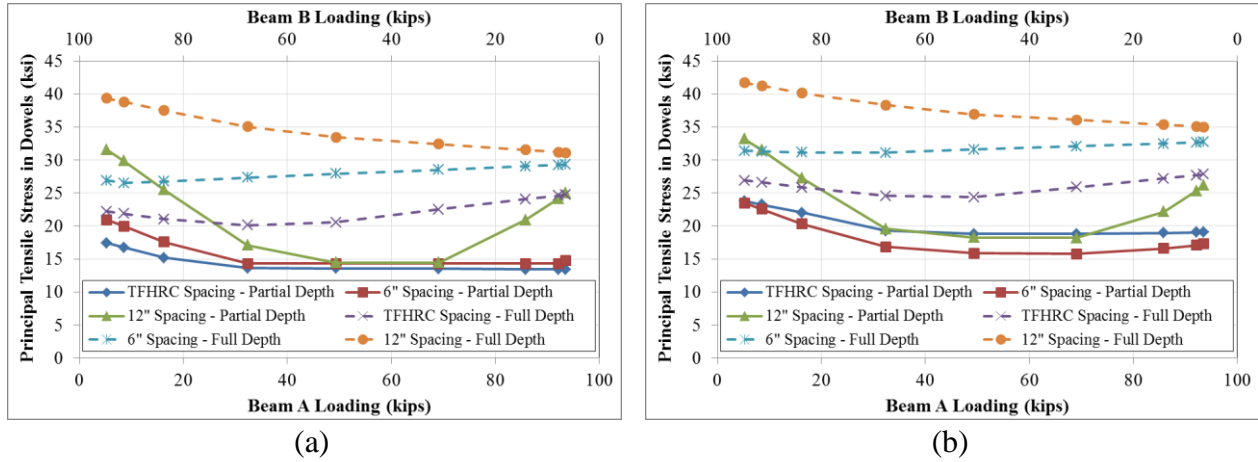
Fig. 11 Transverse dowel bar maximum principle tensile stress comparisons amongst the partial and full depth shear key's varying dowel bar spacing: (a) temperature gradient not applied; (b) temperature gradient applied

MAXIMUM DOWEL FORCE-TO-ULTIMATE DOWEL FORCE RATIO (%)

The performance of the dowels was measured by comparing the maximum dowel force $F_{d,max}$ for each model with the ultimate dowel force F_{du}, at each load increment. The percentage of use, $(F_{d,max}/F_{du}) \times 100$ was computed.The value for $F_{d,max}$, was determined by taking the maximum value for S_{12} from all the dowels in each model (i.e., vertical shear stress in the dowels), and multiplying by the cross section area of the dowel. The ultimate dowel force F_{du} was calculated as the average of the values obtained from Eqs. 2-3 shown below:

$$F_{du} = 1.3\phi^2 \sqrt{f_y f_c'} \qquad \text{(Eq. 2)}$$

and

$$F_{du} = \left[1.35\left(\sqrt{1 + 9\varepsilon^2} - 3\varepsilon\right)\phi^2 \sqrt{f_y f_c'} \right] \qquad \text{(Eq. 3)}$$

where:

F_{du} = ultimate dowel capcity (kips)

$\varepsilon = \dfrac{e}{\phi}\sqrt{\dfrac{f_c'}{f_y}}$ = eccentricity parameter

e = load eccentricity (in)

ϕ = bar diameter (in)

f_c' = concrete compressive stress (ksi)

f_y = steel yielding stress (ksi)

Equations 2 and 3 were obtained from the research performed by Ramussen and Pruijssers, respectively [6][7]. Obtaining a more conservative value for F_{du} was achieved by selecting the value for f_c' as the minimum of the compressive strength between the concrete and the UHPC.

Replacing ϕ = 0.5 in, f'_c = 9.83 ksi, f_y = 60 ksi, and e = 0, the values for F_{du} obtained from Eqs. 2 and 3 were 7.89 kips and 8.20 kips, respectively. Thus, the average value for the ultimate dowel force is F_{du} = 8.04 kips. According to Pruijssers, the value obtained for F_{du} must be multiplied by $[1 - (\sigma/f_y)^2]^{1/2}$ to consider the reduction in the ultimate dowel force due to the axial stress (σ) in the dowels [6]. However, the results showed that the dowel capacity was not considerably altered by utilizing this parameter.

Figure 12(a-b) shows the values obtained in both set of models for the maximum dowel force-to-ultimate dowel force ratio According to the results, the maximum values for $F_{d,max}/F_{du}$ were 18.5% for the partial depth shear key models , and 29.1% for the full depth shear key models. In both cases, the maximum value for $F_{d,max}/F_{du}$ corresponded to the case of 12" dowel spacing, and smaller values were typically obtained for smaller dowel spacing. All values for $F_{d,max}/F_{du}$ were smaller than 100%, allowing to conclude that the ultimate capacity of the dowels for all configurations studied had enough strength to transfer the vertical loads between beams.

(a)   (b)
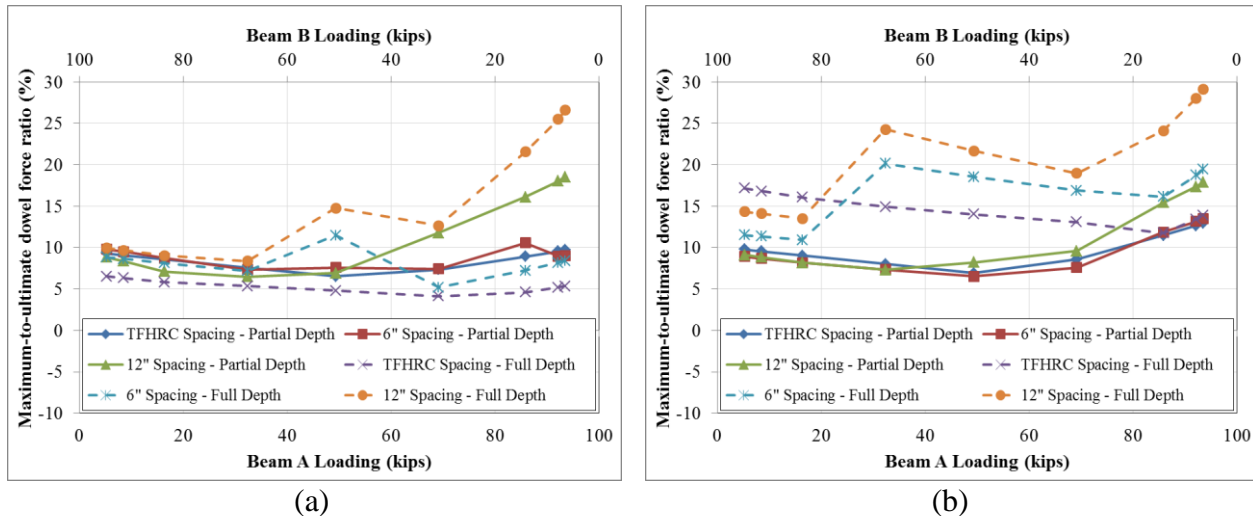
Fig. 12 Maximum dowel force-to-ultimate dowel force amongst the partial and full depth shear key's varying dowel bar spacing: (a) temperature gradient not applied; (b) temperature gradient applied

CONCLUSIONS

1. The principal tensile stress in the shear key remained approximately constant for each load increment. This indicated that, for the UHPC-dowel configurations used in this study, the maximum tensile stresses in shear key were not highly affected by the load differences applied to beams A and B.
2. The principal tensile stress in the shear key increased after a positive temperature gradient was applied to the partial depth shear key. However, for models with full depth shear key, results indicated a decrease in this stresses after a positive temperature gradient was applied.
3. For both partial and full depth shear keys, the principal tensile stress in the shear key was larger as the dowel bar spacing increased.

4. In general, the principal tensile stress in the shear key was larger for models with full depth shear key than it was for models with partial depth shear key.
5. For both partial and full depth shear keys, the principal tensile stress in the dowel bars increased when a positive temperature gradient was included in the models.
6. The principal tensile stress in the dowel bars was larger for models with full depth shear key than it was for models with partial depth shear key. This was because larger tensile stresses were developed in the bottom dowels for the full depth shear key models.
7. The principal tensile stress in the dowel bars was larger as its spacing was increased.
8. The high compressive and tensile strength of UHPC as well as its exceptional adhesive properties with precast concrete elements allowed adequate performance of adjacent box beams subject to differential loads. This was applicable to both models with partial and full depth shear keys. However, results showed that the full depth shear key with 12" transverse dowel bar spacing was inadequate because the principal tensile stresses in the shear key exceeded the UHPC tensile strength.
9. The maximum dowel force for each of the shear key configurations studied in this paper $F_{d,max}$ was smaller than 30% the ultimate dowel force F_{du}. For this reason, it was concluded that, regardless of the shear key configuration used (i.e., partial depth or full depth shear key), the strength of the dowels is sufficient to carry the loads from one beam to the other.
10. Both UHPC-dowel shear key configurations studied experienced satisfactory differential deflections smaller than 0.02 in.
11. After analyzing the performance of both configurations, the authors suggest that using partial depth shear UHPC shear keys with transverse dowel bar spacing of 12" is the most economical solution that satisfies both strength and serviceability requirements for adjacent box-beam bridges.

REFERENCES

1. Precast/Prestressed Concrete Institute (PCI), *The state of the art of Precast/ Prestressed Adjacent Box Beam Bridges* (1st ed.), Chicago, IL, 2009.
2. El-Remaily, A., Tadros, M. K., Yamane, T., and Krause, G, "Transverse design of adjacent precast prestressed concrete box girder bridges," *PCI Journal*, V. 41, No. 4, 1996, pp. 96-113.
3. Graybeal, B, *Behavior of Field-Cast Ultra-High Performance Concrete Bridge Deck Connections Under Cyclic and Static Structural Loading*, Report No. FHWA-HRT-11-023. Federal Highway Administration, McLean, VA, 2010.
4. Graybeal, B., "Construction of Field-Cast Ultra-High Performance Concrete Connections," Technical Note, April 2012.
5. Steinberg, E., Huffman, J., Ubbing, J., & Giraldo-Londoño, O., "Finite Element Modeling of Adjacent Prestressed Concrete Box Beams," *PCI/NBC*, September 2013.
6. Pruijssers, A. F., *Aggregate interlock and dowel action under monotonic and cycling loading*, Delft University Press, Netherlands, 1988.
7. Ramussen, B. H., *Strength of transversely loaded bolts and dowels cast into concrete*, Laboratoriet for Bugningastatik, Denmark Technical University, 1962.
8. AASHTO LRFD *Bridge Design Specification Fifth Edition*, American Association of State Highway and Transportation Officials, Sections 3.12.3-1 & 14.7.6.3.3-1, 2010.

9. Precast/Prestressed Concrete Institute (PCI), *PCI design handbook* (7th ed.), Chicago, IL, 2010.
10. Russell, H. G., & Graybeal, B. A., *Ultra-High Performance Concrete: A State-of-the-Art Report for the Bridge Community*, McLean: Federal Highway Administration, 2013.